YALE JOURNAL OF BIOLOGY AND MEDICINE 92 (2019), pp.397-411.

ORIGINAL CONTRIBUTION

YALE JOURNAL OF BIOLOGY AND MEDICINE
YJBM
CELEBRATING 90 YEARS 1928–2018

Actin Waves and Dynamic Patterning of the Plasma Membrane

Guenther Gerisch*, Jana Prassler, Nelson Butterfield, and Mary Ecke

Max Planck Institute of Biochemistry, Martinsried, Germany

Plasma membrane and underlying actin network are connected to a functional unit that by non-linear interactions is capable of forming patterns. For instance, in cell motility and chemotaxis, cells polarize to form a protruding front and a retracting tail. Here we address dynamic patterns that are formed on a planar substrate surface and are therefore easily accessible to optical recording. In these patterns two distinct areas of the membrane and actin cortex are interconverted at the site of circular actin waves. The inner territory circumscribed by a wave is distinguished from the external area by a high PIP3 content and high Ras activity. In contrast, the external area is occupied with the PIP3-degrading phosphatase PTEN. In the underlying cortex, these areas differ in the proteins associated with the actin network. Actin waves can be formed at zones of increasing as well as decreasing Ras activity. Both types of waves are headed by myosin IB. When waves collide, they usually extinguish each other, and their decay is accompanied by the accumulation of coronin. No membrane patterns have been observed after efficient depolymerization of actin, suggesting that residual actin filaments are necessary for the pattern generating system to work. Where appropriate, we relate the experimental data obtained with *Dictyostelium* to human normal and malignant cell behavior, in particular to the role of Ras-GAP as an enhancer of macropinocytosis, to mutations in the tumor suppressor PTEN, to frustrated phagocytosis, and to the role of coronin in immune cells and neurons.

INTRODUCTION

The subject of this report is the formation of spatial and temporal patterns by the interaction of the plasma membrane with the underlying actin network in eukaryotic cells. Pattern forming activities are required for a diversity of processes including cell motility, cytokinesis, and uptake of particles or fluid by phagocytosis or macropinocytosis. The pattern can form autonomously or is directed by external stimuli. For instance, a motile cell forms autonomously a leading edge and a retracting tail, but where the front is made can be defined by a gradient of chemoattractant provided that receptors on the cell surface recognize the attractant and are coupled by signal transduction pathways to the actin system.

Here we will specify dynamic differentiation of the plasma membrane into microscale territories, focusing on actin wave patterns formed autonomously on the sub-

*To whom all correspondence should be addressed: Dr. Günther Gerisch, Max Planck Institute of Biochemistry, Am Klopferspitz 18, D-82152 Martinsried, Germany; Tel: +49 89 8578-2326, Fax: +49 89 8578-3885, Email: gerisch@biochem.mpg.de.

†Abbreviations: NCLs, neuronal ceroid lipofuscinoses; PIP3, phosphatidyl-inositol-(3,4,5)-trisphosphate; RBD, Ras-binding domain; AIP1, actin-interacting protein 1.

Keywords: PIP3, PTEN, Ras, phagocytosis, coronin, myosin, *Dictyostelium*

Author Contributions: G.G. designed the project and wrote the paper, M.E., N.B., and J.P. conducted the experiments. M.E. and G.G. analyzed the data.

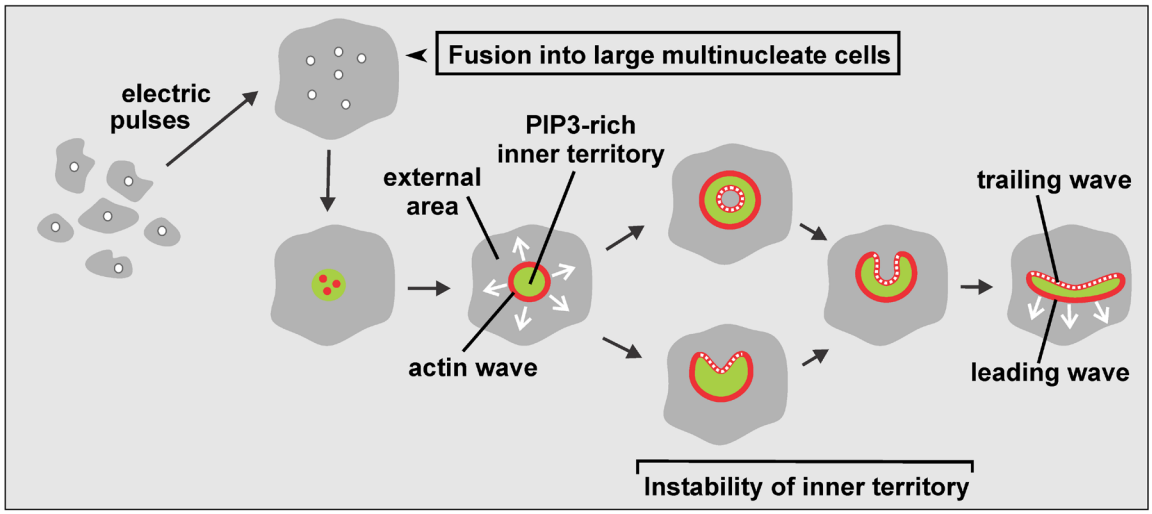

Figure 1. **Diagram of wave patterns recorded in large cells.** Multinucleate cells are produced by electric-pulse induced fusion (top row). In these cells, local increase of PIP3 (green) together with clustering of actin (red) initiates a propagating actin wave that surrounds an expanding PIP3-rich territory (bottom row). Beyond a critical size of about 5 µm radius, the inner territory becomes unstable and is converted into external area. The circular symmetry breaks down such that the inner territory assumes a crescent-like shape. This structure then propagates with a leading segment of an actin wave ahead and a trailing segment behind. Modified from [53].

strate-attached membrane of *Dictyostelium* cells. In these patterns, a circular actin wave separates two distinct areas of the membrane and actin cortex from each other. In the membrane, a PIP3-rich inner territory is distinguished from a PIP3-depleted external area (Figure 1). In the actin cortex, the inner territory is enriched in the Arp2/3 complex that in migrating cells is involved in protrusion of the front region. In the external area, filamentous myosin II and the anti-parallel actin-filament bundling protein cortexillin are accumulated [1], two proteins that typically localize to the cell's tail [2-4]. Analysis of the actin architecture by cryo-electron tomography revealed that the actin waves are characterized by upright filaments branched by the Arp2/3 complex. The data imply that the wave propagates by *de novo* nucleation rather than the elongation of pre-existing filaments [5].

The wave patterns studied can be viewed as planar projections of phagocytic or macropinocytic cups. With phagocytic cups they have in common their formation on a solid substrate surface. In the case of the waves a planar substrate replaces the curved surface of a particle to be taken up. Thus wave formation may be considered as an act of frustrated phagocytosis, an attempt to ingest a particle that is much too large for the phagocyte to engulf [6]. This relates wave formation to the behavior of cells in the immune system. Frustrated phagocytosis is observed when macrophages or granulocytes are exposed to an opsonized surface, such as a planar glass surface coated with antibody or lectin [7,8], or when macrophages attempt to engulf hyphae of *Candida* that are too long to be taken up [9]. With macropinocytic cups the wave patterns have in common their autonomous formation. Their shape is not dictated by the shape of the surface to which the cell adheres; the planar surface does not provide any spatial cues on which the wave patterns could be shaped. Importantly, actin wave formation is enhanced by the same mutation as macropinocytosis, causing the inactivation of a Ras-GAP, the neurofibromin ortholog of *Dictyostelium* [10]. Human neurofibromin regulates neural differentiation and acts as a tumor suppressor. In patients with deficient neurofibromin activity, p21Ras is constitutively active and initiates the tumorigenesis of neurofibromas (reviewed in [11]).

Dictyostelium discoideum is a eukaryotic microorganism capable of surviving under the variable conditions of forest soil. Its peculiarity is the transition from a single-cell to a multicellular stage. *Dictyostelium* cells are professional phagocytes of about the size of a neutrophil. Upon starvation, the cells aggregate by chemotaxis up a cyclic-AMP gradient ultimately forming dormant spores at the head of a fruiting body. Phagocytosis of bacteria and chemotactic movement are primarily based on the actin system in the cell cortex that acts in concert with signal recognition and transduction systems at the plasma membrane. However, regulatory systems, including phosphoninositides in the plasma membrane, small GTPases, and actin-associated proteins are required also in the absence of external stimuli to control localized activities in normal cell motility, such as protrusions formed at the front of the cell and retraction at the tail.

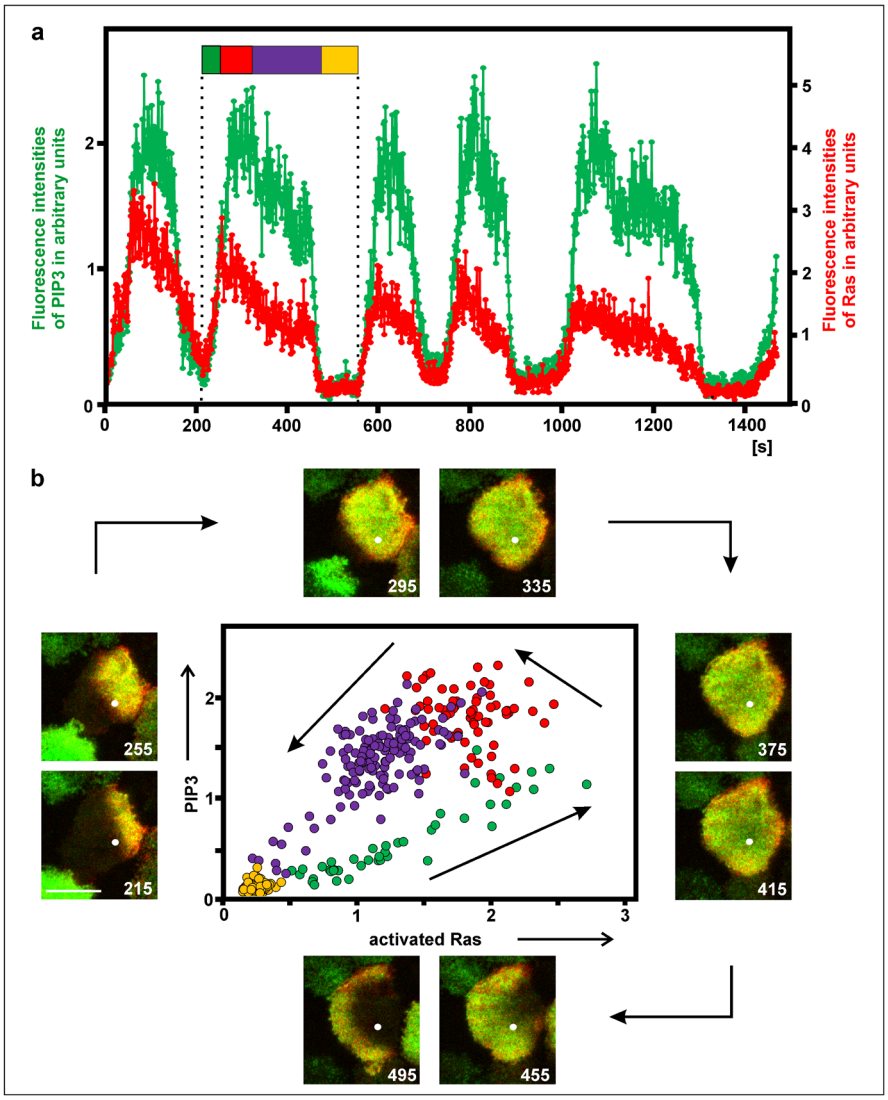

Figure 2. Relation of PIP3 and activated Ras on the substrate-attached membrane. The cell was in the recovery phase after treatment with 5 µM latrunculin A. **a**, fluorescence intensities of GFP-PHcrac as a label for PIP3 (and PI(3,4)P2) (green) and of mRFP-RBD for activated Ras (red) measured at a single point. The flag demarcates one cycle of PIP3 accumulation and Ras activation, the color code corresponding to the phases in the diagram of (b). For reasons of clarity, the normalized fluorescence intensities were plotted at different scales. **b**, TIRF images at intervals of 40 s and phase diagram of the PIP3 and Ras cycle that is indicated by the flag in (a). The white dot in the images indicates the point of fluorescence measurement. Bar in the first frame, 10 µm. The phase diagram shows the concomitant rise of PIP3 and Ras activity (yellow to green transition), the fall of Ras activity while PIP3 is still increasing (red), and the decline of both PIP3 and Ras activity (blue).

Because the molecular setups for basic cellular functions such as motility and endocytosis are largely conserved, *Dictyostelium* has proved to be suitable as a genetically tractable model organism to elucidate the molecular basis of chemotaxis [12,13], phagocytosis [14], and macropinocytosis [15,16] in view of corresponding human diseases [17]. For example, *Dictyostelium* contains homologs of 11 of the 13 human genes associated with neurodegeneration causing Batten disease, a group of neuronal ceroid lipofuscinoses (NCLs) [18]. These storage disorders are due to lysosomal dysfunction. The *Dictyostelium* homologs of human genes for NCL proteins encode, among others, six homologs of a lysosomal serine protease (TPP1), which limits autophagy [18,19], and two of the *Dictyostelium* homologs have been shown to bind to the Golgi pH regulator [20].

For optical recording by confocal or TIRF microscopy, the wave patterns have the advantage of being formed on a planar substrate surface. Questions to be addressed are: what are the molecular players in the autonomous formation of wave patterns and what are the regulatory circuits that are responsible for spatial membrane differentiation? For a comprehensive view of the interactions between membrane and actin cortex, we outline here the relation of membrane-bound active Ras, phosphatidyl-inositol-(3,4,5)-trisphosphate (PIP3), the PIP3-degrading PI3-phosphatase PTEN, the single-headed motor protein myosin IB, and the actin-filament destabilizing protein coronin in actin-wave patterns that are generated on the substrate-attached plasma membrane of *Dictyostelium* cells.

The proteins and the phosphatidylinositide studied here as constituents of the wave pattern have human counterparts of medical relevance, as illustrated by the following spotlights. Members of the Ras family of small GTPases act as molecular switches [21] that may become oncogens when mutated to constitutively active forms; mutations in the human genes for KRas, HRas, or NRas are frequently linked to lung, gastrointestinal, and pancreatic cancer [22]. The Ras-binding domain (RBD) of a human effector, Raf1, recognizes the activated, GTP-bound, and membrane-associated state of *Dictyostelium* RasG [23].

PIP3 is a signal transducer to the actin cytoskeleton that in *Dictyostelium* as well as in human cells has been implicated in chemotaxis [24,25] and phagocytosis [26,27]. PIP3 is synthesized from PI(4,5)P2 by class I PI3-kinases. Activating mutations in these lipid kinases contribute to tumor progression through multiple effector pathways [28], one of them linked to the metastasis-promoting activity of invadopodia [29].

Human PTEN is a dual lipid and protein phosphatase known as a tumor suppressor [30,31] and a metabolic regulator [32]. Most cancer-associated PTEN mutations are associated with the catalytic residues, others with membrane-binding sites or with decreased stability of the protein [33].

Dictyostelium as well as human cells contain a heterogeneous group of unconventional myosins that differ from conventional myosins by their inability to form bipolar filaments [34] and fulfil a variety of functions in muscle and non-muscle cells [35,36]. Myosin IB is one of seven members of the myosin I sub-family in *Dictyostelium* [37], and partially overlaps in function with myosins IC and ID [38]. A short sequence of basic and hydrophobic amino acids in the tail region mediates binding of myosin IB to acidic phospholipids in the membrane [39]. The localization of myosin IB in actin waves corresponds to its position at the border of phagocytic cups [26].

Coronin discovered in *Dictyostelium* by de Hostos *et al*. [40] is an actin-binding protein involved in cell motility, cytokinesis, and phagocytosis [41,42]; it was coined with reference to its prominent localization to crown-shaped endocytic cups. The coronin is a WD40-repeat protein, forming a 7-bladed β-propeller as an actin interacting domain [43]. In *Dictyostelium*, coronin acts together with actin-interacting protein 1 (Aip1) in depolymerizing actin filaments [44]. In *Saccharomyces cerevisiae*, coronin indirectly regulates the depolymerization of actin: it binds preferentially to ATP-actin and thus prevents early severing of the filaments by cofilin [45].

The *Dictyostelium* coronin turned out to be the prototype of a family of proteins that in human cells is represented by seven paralogs [46]. Mammalian coronin 1 functions in the immune system by controlling T cell homeostasis, and in macrophages it is hijacked by *Mycobacterium tuberculosis* to enable survival of the pathogenic bacteria in phagosomes [47]. Coronin 1 depletion in mice results in tolerance of allografts but maintains immune responses to microbial pathogens [48]; with comments in [49]. In the peripheral nervous system, coronin 1 plays a role in nerve-growth-factor signaling by preventing the signaling endosome from lysosomal fusion [50], a function similar to the role the coronin plays in phagocytosis.

RESULTS

Relation of PIP3 to Activated Ras

Pattern formation on the substrate-attached plasma membrane is primarily based on the activation of Ras and the synthesis of PIP3, two events that are coupled to each other and result in signal transduction to the actin system. To quantify the temporal relationship of these events, PI(3,4,5)P3 (and PI(3,4)P2) were labeled with GFP-PHcrac, and activated Ras with mRFP-RBD. Recording the fluorescence intensities at a single point on the substrate-attached cell membrane showed that both labels increased in parallel (Figure 2a). The two labels indicated, however, one difference in the temporal pattern of activated Ras and PIP3: the decline began first in Ras, uncoupled from PIP3, which reached its peak later. In the phase diagram of one cycle shown in Figure 2b, the green labeled dots correspond to the parallel increase of Ras activation and PIP3, and the red labeled ones to the delayed decrease of PIP3. There are two phases in the decline of Ras activity and, even more prominently, in PIP3. The cluster of violet dots in the phase diagram reflects the phase of slow decline, which is followed by the rapid fall of both Ras activity and PIP3.

Alternation of PTEN Binding and Ras Activation

PIP3 is degraded by the PI3-phosphatase PTEN, which requires membrane binding to become activated

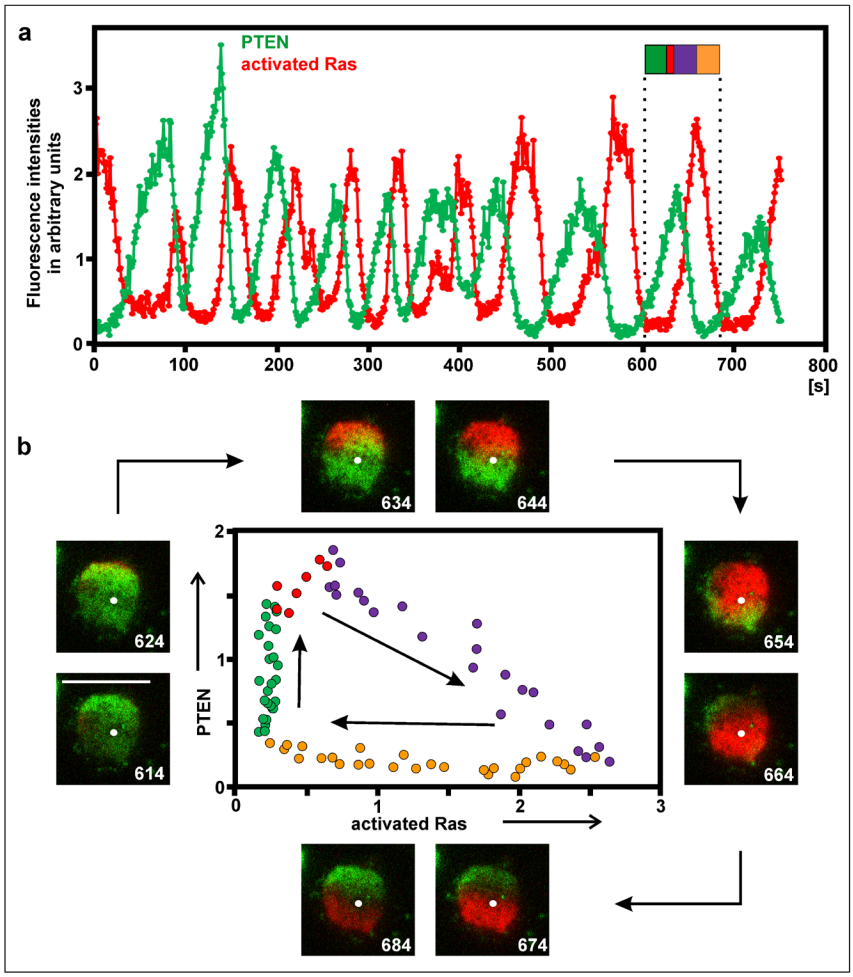

Figure 3. Relation of PTEN and activated Ras on the substrate-attached membrane. This figure is directly comparable to Figure 2. Cells were incubated with 5 µM latrunculin A to moderately inhibit actin polymerization. **a**, fluorescence intensities of GFP-PTEN (green) and mRFP-RBD as a label for activated Ras (red) measured at a single point. The flag demarcates one cycle of PTEN accumulation and Ras activation, the color code corresponding to the phases in the diagram of (b). The white dot indicates the point where fluorescence intensities were measured. The fluorescence intensities were normalized by setting the average intensity in each channel to 1. Figure 3a relates to Video 1. **b**, details of a single PTEN and Ras cycle as indicated by the flag in (a). TIRF images display PTEN (green) and activated Ras (red) on the substrate-attached surface of a cell at intervals of 10 s, beginning on the left with the 614-s frame. Bar in the 614-s frame, 10 µm. The phase diagram shows the increase of PTEN binding during the absence of activated Ras (green), the onset of Ras activation during a phase of continued PTEN increase (red), the rise of Ras activation while PTEN decoration declines (blue), and the fall of activated Ras in the absence of PTEN (yellow).

[51]. As shown in Figure 3a and Supplemental Video 1, peaks of PTEN occupancy alternate with peaks of Ras activation on the membrane. The precise relationship of PTEN binding to the activation of Ras is displayed in the phase diagram of one cycle in Figure 3b. Characteristics of the phase relationship are the beginning of Ras activation during the continued increase of PTEN binding (red labeled dots in the phase diagram), the gradual disappearance of PTEN during further increase of Ras activation (blue), the subsequent decline of activated Ras in the absence of PTEN (yellow), and the increase of PTEN binding in the absence of activated Ras (green). These data are in accord with a report by Fukushima *et al*. [52]. They are consistent with a role of activated Ras in removing PTEN from the membrane, and with a Ras cycle that is independent of PTEN fluctuations.

Leading and Trailing Waves are Formed at Positive and Negative Ras Gradients

Actin waves propagate at the border of the territory rich in PIP3 and activated Ras. When the territory expands, the actin waves are formed during the increase of PIP3 as well as activated Ras, suggesting a coupling of

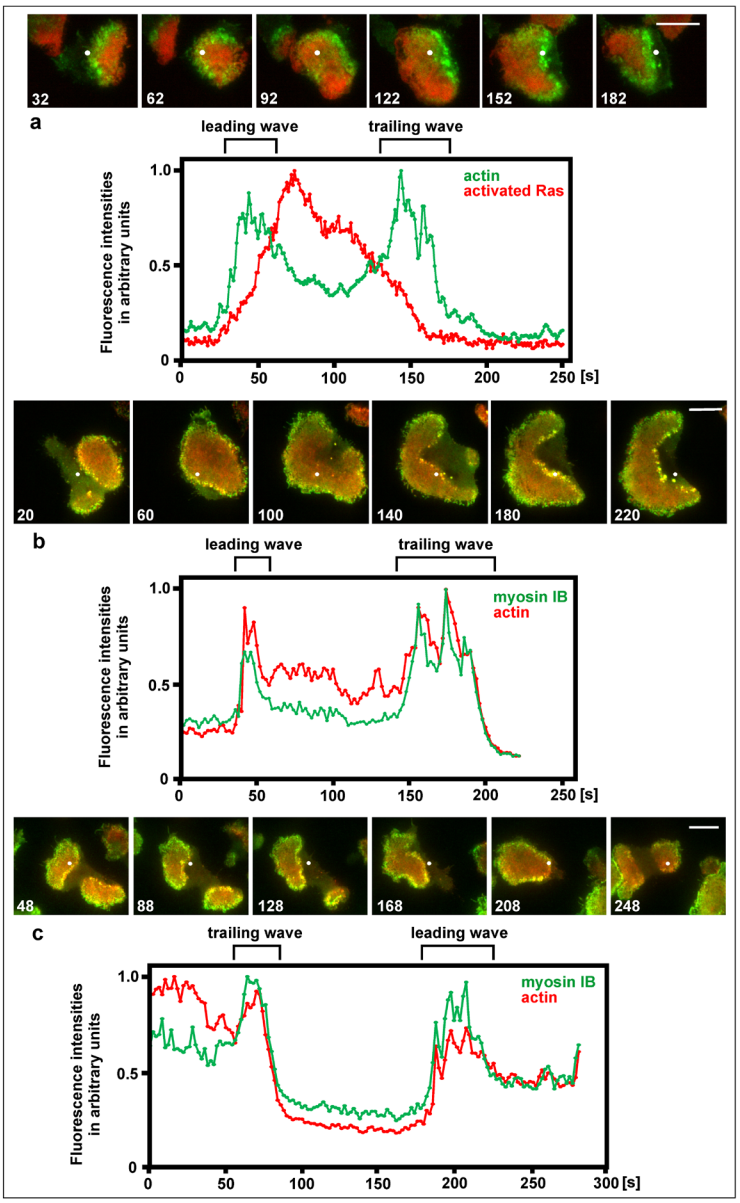

Figure 4. **Actin waves formed at both the rise and decline of activated Ras, and recruitment of myosin IB to both the leading and trailing waves.** The figure shows three cells forming leading and trailing waves. For each cell, series of TIRF images are shown, and scans of fluorescence intensities measured at a single point of the substrate-attached cell surface. The white dot in the image series indicates the point of recording fluorescence intensities for the scans displayed beneath each series. **a**, a cell expressing mRFP-RBD as a label for activated Ras (red) and LimEΔ-GFP for filamentous actin (green). The cell recovered from treatment with 5 µM latrunculin A. In the scans of fluorescence intensities, high Ras activity characterizes the inner territory, peaks of the actin label represent the two actin waves. The first wave is formed during transition from external area to inner territory, the second wave during reversal of inner territory to external area. At the 32-s and 62-s frames of the image series, a first actin wave passes the point of recording fluorescence intensities, at the 92-s up to the 122-s frame inner territory occupies the point, a second actin wave passes at the 152-s frame, and finally external area occupies the point at the 182-s frame. Figure 4 a relates to Video 2. **b and c**, large cells produced by electric-pulse induced fusion that expressed mRFP-LimEΔ as a label for filamentous actin (red) and GFP-myosin IB (green). In (b) a leading wave where external area is converted into inner territory, is followed by a trailing wave where the opposite conversion occurs. In (c) a wave reverts the direction of propagation; first acting as a trailing wave and subsequently, after the reversal of direction, as a leading wave. Time in the images is given in seconds consistent with the corresponding scans beneath each image series. Bars, 10 µm.

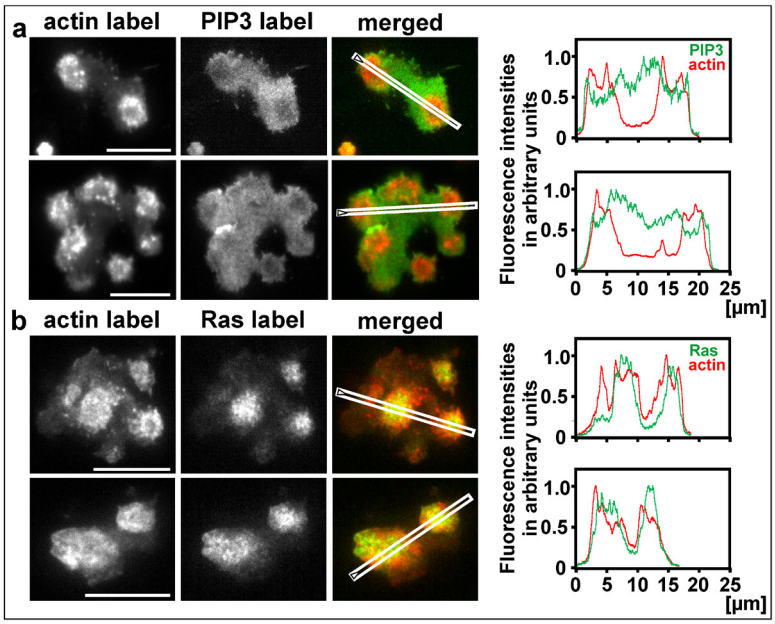

Figure 5. Actin wave formation in the absence of PTEN. The cells were produced by electric-pulse induced fusion of PTEN-null cells. Line scans on the right correspond to the images on the left, where the scan directions are indicated. **a**, two cells expressing mRFP-LimEΔ for filamentous actin and GFP-PHcrac for PIP3. In the merged images and the scans, the actin label is shown in red and the PIP3 label in green. **b**, two cells expressing mRFP-LimEΔ for filamentous actin and GFP-RBD for activated Ras. In the merged images and the scans, the actin label is shown in red and the Ras label in green. Bars, 10 µm.

one or both of these membrane-bound signaling factors to the actin polymerizing machinery. However, there is no monotonic dependence of actin polymerization on these factors in the membrane: at the back of the wave, actin polymerization is down regulated in the presence of high PIP3 and activated Ras.

Since the inner territory has a limited lifetime, it is eventually converted into external area [53]. During this conversion the inner territory shrinks and a trailing wave follows its border (Figure 1). This trailing wave is formed in a zone where PIP3 and activated Ras are decaying rather than increasing (Figure 4a and Supplemental Video 2). The question is then how actin polymerization and depolymerization are regulated during the conversion from inner territory to external area, such that a trailing wave is formed.

As one piece of evidence that the organization of trailing waves is comparable to that of leading waves, we determined the localization of myosin IB, a single-headed motor protein that co-localizes with sites of actin polymerization in waves [2,39,54]. To measure fluorescence intensities of GFP-myosin IB together with mRFP-LimEΔ as a reference for filamentous actin, we have chosen points which were traversed in succession by a leading and a trailing wave. Figure 4b shows the common case of a trailing wave following a leading one at a distance determined by the lifetime of the inner territory (see scheme in Figure 1). Figure 4c shows an example of wave reversal: a trailing wave turning into a leading one. In both cases, myosin IB is recruited to the leading as well as the trailing wave.

Actin Waves Linked to Ras Activation in the Absence of PTEN

The question of whether actin waves are formed at the border of a territory occupied by activated Ras or whether they require the border of a PIP3-decorated territory was addressed using PTEN-null cells, in which PIP3 no longer forms waves [52]. The PTEN-null cells formed wave-like circular assemblies of filamentous actin without differentiation of the substrate-attached membrane into a PIP3-rich inner territory and a PIP3-depleted external area. The entire substrate-attached cell surface was decorated with PIP3, and if there was a heterogeneity, the PIP3 label was slightly weaker beneath the actin assemblies (Figure 5a). In contrast to PIP3, Ras was activated in discrete territories, and these territories turned out to be the sites of actin polymerization (Figure 5b). As a caveat we wish to add that the waves did not propagate normally in the absence of PTEN, which argues for a contribution of PIP3 to the dynamics of the wave pattern.

Sub-threshold Fluctuations in the Actin System and the Initiation of Propagating Waves

Actin wave formation is not only regulated by sig-

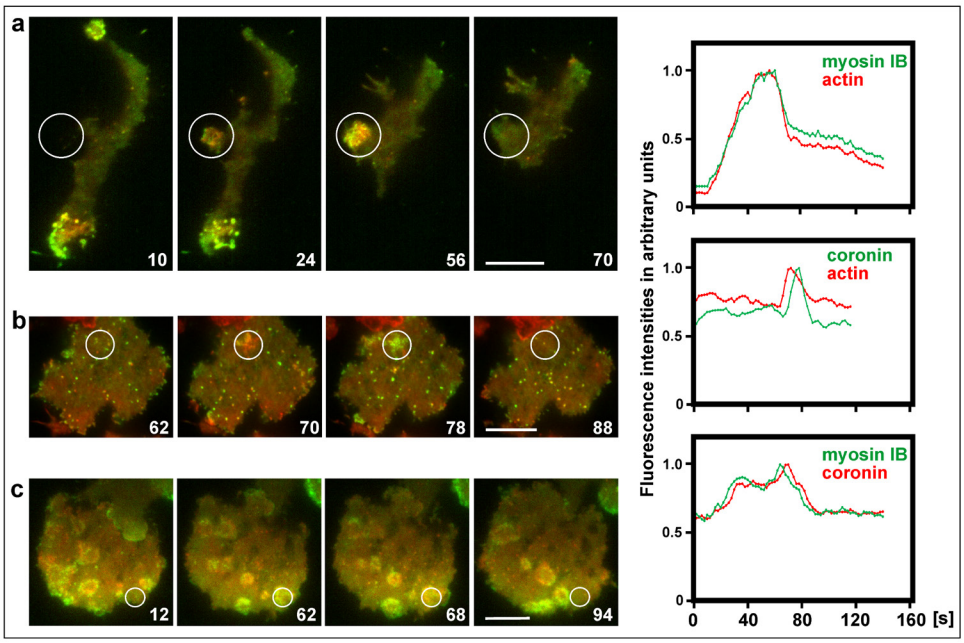

Figure 6. Sub-threshold fluctuations in the actin system. TIRF images show actin structures on the substrate-attached surface of large cells produced by electric-pulse induced fusion. The cells expressed different pairs of fluorescent proteins. Left panels: merged fluorescence images. Right panel: Scans of fluorescence intensities within the encircled area of the images. **a**, mRFP-LimΔ label for filamentous actin (red) and GFP-myosin IB (green). In the first image, most of the measured area was still in the extracellular space, and only later the cell formed a protrusion into this area. **b**, actin label as in (a) (red) and coronin-GFP (green). Figure 6 b relates to Video 3. **c**, mRFP-coronin (red) and myosin IB (green). Time is indicated in seconds. Bars, 10 µm.

nals that stimulate actin polymerization but also by factors that turn it down. One of these factors is coronin [2]. Coronin localizes to various sites of actin disassembly in *Dictyostelium* cells [55-58] and is, together with actin interacting protein 1 (Aip1), part of the disassembly machinery [44]. Accordingly, coronin localizes to sites of actin disassembly at the roof and the back of a wave [2].

Previous work on the wave-forming network as an excitable system has focused on phosphoinositide regulation, showing that locally PTEN declines and PIP3 rises, and that a propagating wave is initiated only if this change in the membrane exceeds a threshold [59]. The data presented in Figure 6 extend these studies to sub-threshold events on the level of the actin cytoskeleton, which fail to result in the initiation of a propagating wave. These local increases of actin polymerization at the substrate-attached membrane are accompanied by the accumulation of myosin IB, and they disassemble while coronin becomes dominant (Figure 6a, frames 24, 56, Figure 6b, frames 70, 78, and Figure 6c, frames 62, 68) (see also Supplemental Video 3).

Only if actin polymerization momentarily escapes the down-regulation, the actin assembly crosses the threshold and a propagating wave is initiated. By expanding, the circular wave leaves behind the inner territory rich in PIP3 and activated Ras. In the propagating waves, coronin again accompanies the increase in actin polymerization and the recruitment of myosin IB, indicating that the accumulation of filamentous actin is restricted by depolymerization. Characteristic of the propagating wave fronts are fluctuations in the timing and quantity of coronin recruitment relative to the actin or myosin IB peaks (Figure 7a, frames 28, 32, Figure 7b, frames 40 – 146) (see also Supplemental Video 4). Most often, coronin recruitment slightly lags behind the peaks of actin or myosin IB (Figure 7a, frames 84 – 130, Figure 7b, frames 86, 98).

Coronin is Associated with the Extinction of Colliding Waves

The recruitment of coronin to decaying actin structures is most evident during the collision of two waves. Colliding actin waves usually extinguish each other; only occasionally one wave continues to propagate while the other one is extinguished [53]. The mutual extinction of two colliding actin waves is accompanied by a peak of coronin recruitment (Figure 8a, c, and Supplemental Video 5). The time of this peak coincides with a phase of rapid actin disassembly (Figure 8b), and with the decline of myosin IB recruitment (Figure 8d).

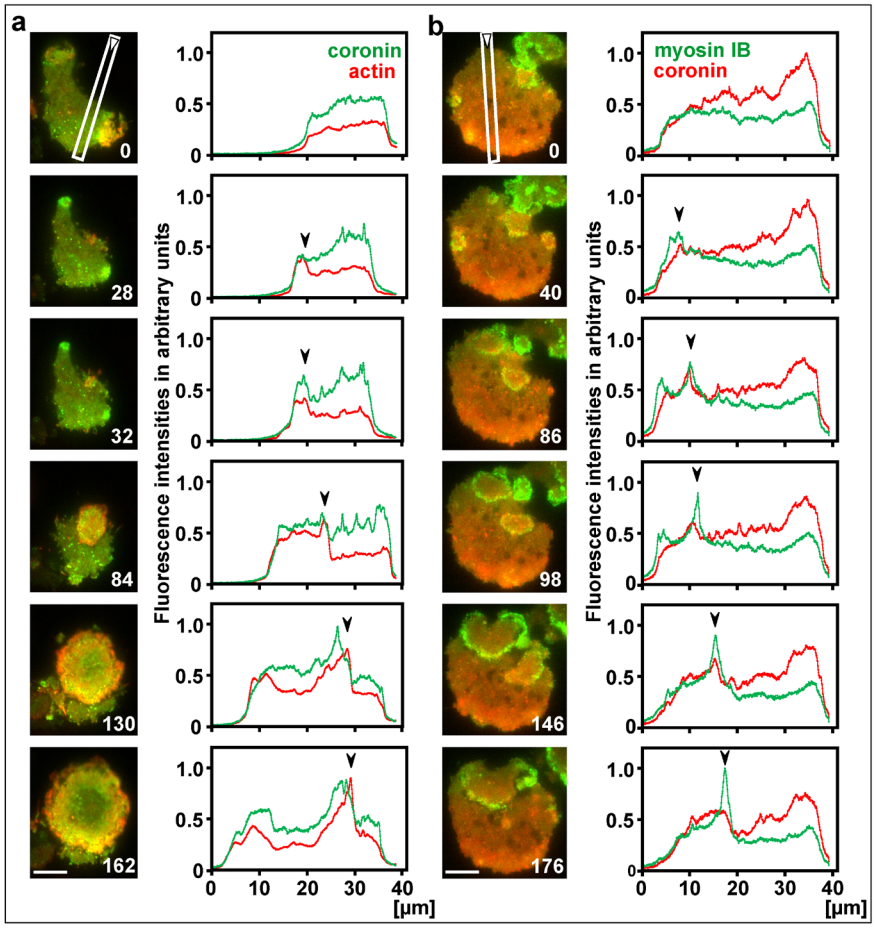

Figure 7. Initiation of propagating waves. Large cells were produced by electric-pulse induced fusion and imaged by TIRF microscopy. **a**, a cell expressing mRFP-LimEΔ as a label for filamentous actin (red) and coronin-GFP (green). Figure 7 a relates to Video 4. **b**, a cell expressing GFP-myosin IB (green) and mRFP-coronin (red). Right to the images, scans of fluorescence intensities are plotted along the lines and directions indicated in the first image of each series. In the plots, waves propagate from left to right, with the peak positions of actin or myosin IB indicated by arrowheads. Time in seconds is indicated in the images. Bars, 10 µm.

Are the Membrane Patterns Dependent on Filamentous Actin?

Actin wave formation linked to membrane patterns is facilitated by pre-treatment with latrunculin A, an inhibitor of actin polymerization. During the recovery phase after washout of the inhibitor, the cells profusely form waves [60]. We wish to point out, however, that this pre-treatment is not essential; in particular, large cells produced by electric-pulse induced fusion consistently generate waves without having been exposed to latrunculin A [53].

The question of whether polymerized actin is required for the membrane patterns to be formed can be addressed by efficient depolymerization. In cells incubated with 5 µM latrunculin A, membrane patterns persisted (Figure 3). However, inspection of electron-tomograms revealed actin filaments persisting under these conditions, even though the cells were rounded up and showed pearling as a result of insufficient stabilization of the membrane by the underlying actin network [61]. These data show that Ras activation is independent of a functional actin cytoskeleton [52], but they do not provide proof that it is independent of any filamentous actin.

At an extremely high latrunculin A concentration of 30 µM, the results depended on details of the incubation, since Ras and PTEN patterns became strongly light sensitive. At reduced illumination, activated Ras still formed mobile patches at the membrane. Since latrunculin A sequesters profilin-actin complexes, the possibility remains that a profilin-independent backup mechanism of actin polymerization, for instance a formin-dependent one, is responsible for persistence of the membrane patterns. To exclude this possibility, we applied 10 µM latrunculin A

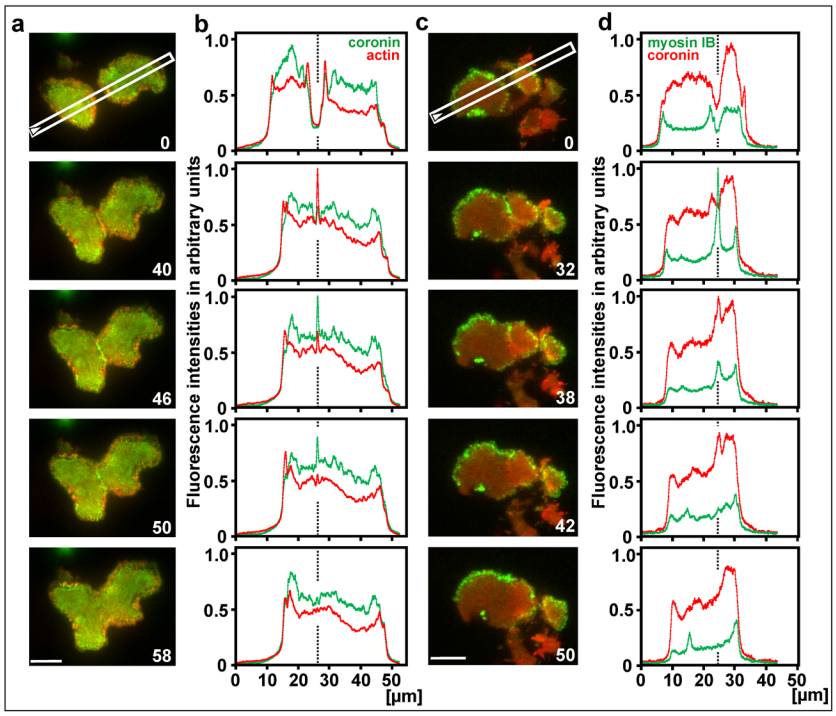

Figure 8. Coronin and myosin IB in colliding waves. a, c, TIRF images of large cells produced by electric-pulse induced fusion, the first frame showing positions of the line scans plotted in (b,d). The cell in (a) expressed coronin-GFP in (green) and mRFP-LimEΔ for actin (red); the cell in (c) expressed mRFP-coronin (red) and GFP-myosin IB (green). Figure 8 c relates to Video 5. **b, d**, scans of fluorescence intensities at stages before, during and after wave collision. A dotted line indicates the site of collision. In (b), an actin peak in the 40-s panel is followed by a coronin peak in the 46-s panel. In (d), a myosin IB peak in the 32-s panel is followed by a coronin peak in the 38-s panel. Note that in (a,b) coronin-GFP, in (c,d) mRFP-coronin has been used. Time in seconds for (a,b) and (c,d) is indicated in the images. Bars, 10 µm.

together with 10 µM cytochalasin A, which blocks the elongation of actin filaments by binding to their plus-end. This combined blocking activity abolished the RBD and PTEN patterns, consistent with their requirement for a minimum of polymerized actin.

DISCUSSION

Activities Associated with Actin Waves

Dictyostelium cells have to migrate in their natural environment of irregular geometry to find their path between soil particles. The actin wave patterns studied are formed in contact with a substrate surface, and can be used to explore the response of cells to a 3-dimensional environment. Upon exposure to a perforated substrate surface, cells apply force to try and protrude into the holes of the substrate specifically at the sites of the waves and the inner territory that they encircle [62]. Accordingly, the waves can be considered as structures analogous to invadopodia of mammalian cells that explore gaps in the substrate to penetrate into. Invadopodia equipped with metalloprotease are responsible for the penetration of metastasizing cancer cells into the spaces between tissue cells [63,64].

The three-dimensional environment through which the cells have to maneuver raises the question as to how attachment to the various surfaces is coordinated. To address this question, *Dictyostelium* cells were confined between two parallel surfaces using the actin waves as markers for engagement of the cells with a substrate surface [65]. Under these conditions, the cells had the choice of either to form waves simultaneously on the two competing surfaces or to alternate between them. In fact, the cells switched periodically from one surface to the other, thus exerting force at regular intervals into opposite directions.

Molecular Basis of Wave Patterns

The actin-wave forming cells provide a possibility of studying by optical techniques the dynamics of large-scale patterns that are generated spontaneously at the interface of the plasma membrane and the underlying actin network. Both PIP3 and activated Ras have a limited lifetime in these patterns, which implies that persistence

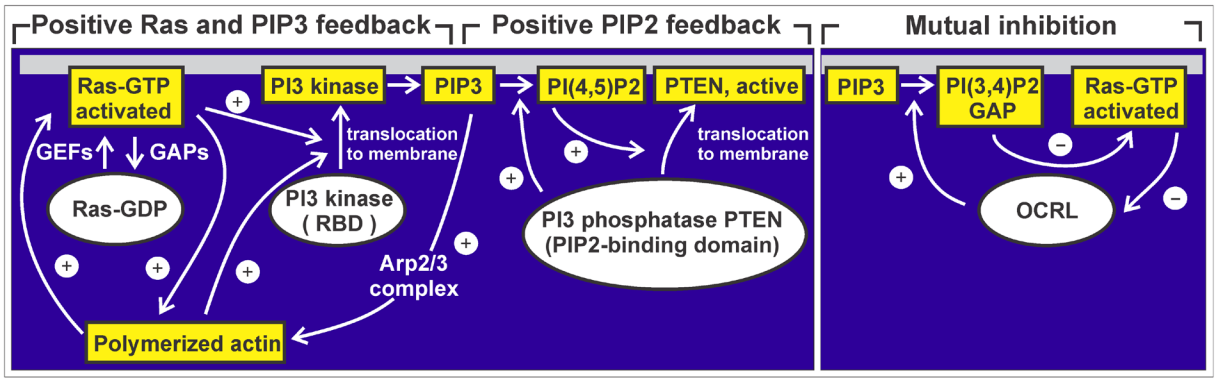

Figure 9. **Diagram of control circuits relevant to pattern generation in membrane and actin cortex.** Ras switches from a GDP-bound inactive to a GTP-bound activated state at the membrane. Two other components involved shuttle between a cytoplasmic and a membrane bound state: Three PI3 kinases of *D.discoideum* have a Ras-binding site (RBD) to interact with membrane-bound activated Ras [80]. The PTEN of *D.discoideum* harbors two membrane-binding sites, one of them specific for its product PIP2, the other negatively regulated by phosphorylation. On the right, mutual inhibition of PI(3,4)P2 and Ras is diagramed, involving Ras-GAP and a *Dictyostelium* ortholog of the human PI5-phosphatase OCRL (Lowe oculocerebrorenal syndrome protein). Compiled from Li et al. [67], Sasaki et al. [70], Vazquez et al. [71], and van Haastert et al. [81].

of the "excited state" of the inner territory is restricted (Figure 1). We show that in the actin waves, PIP3 and activated Ras rise in parallel, but that Ras activity begins to decline before PIP3 stops rising (Figure 2). Therefore, it appears unlikely that in the control circuit responsible for pattern formation, PIP3 sets the signal for the maintenance of Ras activity. This result is in accordance with data indicating that Ras is upstream of PI3-kinase [66]. The premature decline of Ras activity is also consistent with the inhibition of Ras by PI(3,4)P2, a degradation product of PIP3 [67].

Remarkably, both the rise and the fall of PIP3 and Ras activity is accompanied by an actin wave. At the leading wave, external area is converted into the PIP3-rich inner territory, while at the trailing wave propagating in the same direction, inner territory is converted into external area. This scenario implies that in the leading waves actin preferentially polymerizes in a zone of low Ras activity and depolymerizes at high Ras activity, whereas in the trailing waves the opposite is the case. In Figure 4b we show that myosin IB is recruited not only to leading waves, as reported previously, but also to the trailing waves. With its tail, this single-headed motor protein joins the actin network to the membrane [39]. Based on its motor activity, myosin IB might facilitate the incorporation of actin subunits into growing actin filaments at their membrane-apposed plus-end [2]. We are left with the question: what are the signals that determine the assembly of actin and myosin IB not only at sites where PIP3 is synthesized and Ras activation is increasing, but also where PIP3 is degraded and Ras becomes inactivated?

The actin waves encircle a territory that is rich in PIP3, whereas the external area is decorated with the PIP3-degrading phosphatase PTEN. Previous work has shown that PIP3 declines before the increase of PTEN-binding to the membrane [59]. Knoch *et al*. [68] have modeled this relationship based on the assumption that PTEN switches between states of high and low activity. An alternative would be the presence of a second PI3-phosphatase [69].

We emphasize the interplay of positive and negative controls of actin polymerization in wave initiation and propagation and that coronin plays a role in the latter. As a negative regulator, coronin is recruited to sub-threshold assemblies of actin that fail to initiate a wave (Figure 6b), and is a hallmark of wave extinction at sites where two waves collide (Figure 8a, b, frames 46, 50, and Figure 8c, d, frames 38, 42).

Efficient inhibition of actin polymerization by a combination of latrunculin and cytochalasin prevented the formation of Ras and PTEN patterns at the membrane. Requirement of an actin network for the generation of the membrane patterns is supported by the sensitivity of wave formation to the formin inhibitor SMIFH2. This inhibitor has been shown to abolish force generation by actin waves [62]; at a concentration as low as 1 µM it reversibly inhibits actin wave formation and PIP3 accumulation at the membrane (unpublished results). These data are in accordance with previous findings indicating that the activation and localization of PI3-kinase to the membrane depends on polymerized actin [66,70].

In Figure 9, data from different sources are compiled to illustrate cross-talk between membrane and actin cor-

tex in pattern generation. Taken together, the data reveal that membrane and actin cortex are linked to each other by several feedback circuits. A positive feedback involving Ras and PI3-kinase is antagonized by a positive feedback of PTEN recruitment to the membrane, which results in degradation of PIP3. PTEN binds to PI(4,5)P2, the product of its own activity, and the membrane-binding is required to activate PTEN [51,71]. A third regulatory feedback system results in mutual inhibition of PI(3,4)P2 and Ras [67]. In this system, a PI5-phosphatase converts PIP3 to PI(3,4)P2, which binds Ras-GAP and thereby recruits this Ras inactivator to the membrane. The results presented in this paper document the phase relationships of components in the coupled feedback circuits and emphasize the fact that actin waves are linked not only to the rise of Ras activity and PIP3, but also to their fall.

MATERIALS AND METHODS

Cell Culture and Sample Preparation for Light Microscopy

Cells of *D. discoideum* strain AX2-214 expressed mRFP-LimEΔ or LimEΔ-GFP [72,73] as an actin probe together with either an mRFP-Raf1-RBD construct, the minimal Ras-binding domain (RBD) of human Raf proto-oncogene serine/threonine-protein kinase (Raf-1) [74], superfolding-GFP-PHcrac [75] as a label for PIP3, coronin-GFP, mRFP-coronin [42], or GFP-myosin IB [39]. Expression of PTEN-GFP [76], a label for PI3-phosphatase was combined with mRFP-Raf1-RBD, and GFP-myosin IB with mRFP-coronin. PTEN-null cells [77,78] were transfected with mRFP-LimEΔ together with superfolding-GFP-PHcrac or GFP-Raf1-RBD.

The cells were cultivated in Petri dishes with nutrient medium containing 10 µg/ml of blasticidin (Invitrogen, Life Technologies, Grand Island, NY, USA) and 10 µg/ml of G418 (Sigma-Aldrich, St. Louis, Missouri, USA). They were harvested from the Petri dishes and washed twice in 17 mM K/Na-phosphate buffer pH 6.0 (PB). An aliquot was pipetted in a HCl-cleaned cover-glass bottom dish (FluoroDish, WPI INC., Sarasota, FL, USA) with PB for TIRF imaging. Waves were initiated either by adding 5 µM Latrunculin A (Invitrogen, Thermo Fisher Scientific, Waltham, MA, USA) and (except for Figure 3) exchanging it for PB after 15 min, or they were spontaneously formed in large cells produced by electric-pulse induced fusion [53].

Image Acquisition and Data Analysis

For dual-color TIRF imaging of the substrate-attached membrane region, a GE DeltaVision Elite system based on an OLYMPUS IX-71 inverted microscope, with an OLYMPUS TIRF 100X/1.49 UAPON objective and a PCO sCMOS 5.5 camera or alternatively an Olympus IX 71 microscope equipped with an 150x UApo NA 1.45 TIRF objective and an Andor iXon 897 Ultra EM-CCD camera at 21 ±2°C were used.

Images were analyzed using the image processing package Fiji (http://Fiji.sc/Fiji) developed by Schindelin *et al.* [79] on the basis of ImageJ (http://imagej.nih.gov/ij). Data of line scans and point scans were imported into an excel sheet and processed further.

SUPPLEMENTARY MATERIAL

Supplementary Video 1. **Activated Ras and PTEN patterns on the substrate-attached membrane of a cell incubated with 5 µM latrunculin A.** This video relates to Figure 3a, b, showing activated Ras labeled in red and PTEN colored in green. The white dot indicates the point of scanning fluorescence intensities in the figure. Exposure time for both channels is 50 ms. Frame-to-frame interval is 1 s. Bar, 10 µm.

Supplementary Video 2. Leading and trailing waves in TIRF images showing labels for activated Ras (red) and filamentous actin (green). This video relates to Figure 4a. In the images on the left, the position of the line scans of fluorescence intensities is indicated. These scans are shown on the right. Exposure time for both channels is 100 ms. Frame-to-frame interval is 1 s. Bar, 10 µm.

Supplementary Video 3. Fluctuations of filamentous actin (red) and coronin (green) on a substrate-attached cell surface. This video relates to Figure 6b. The circle surrounds a cluster of actin assembly that is followed by coronin accumulation. The cell surface is populated by numerous clathrin-coated pits that are being internalized [58]. Exposure time is 100 ms for the red channel, and 300 ms for the green channel. Frame-to-frame interval is 2 s. Bar, 10 µm.

Supplementary Video 4. Initiation of a propagating wave with filamentous actin shown in red and coronin in green. This video relates to Figure 7a. In the images on the left, the position of the line scans of fluorescence intensities is indicated. These scans are shown on the right. Exposure time is 100 ms for the red channel, and 200 ms for the green channel. Frame-to-frame interval is 2 s. Bar, 10 µm.

Supplementary Video 5. Mutual extinction of colliding waves. In the zone of collision, first myosin IB (green) is enriched, subsequently coronin (red) is accumulated. This video relates to Figure 8c, d. In the images on the left, the position of the line scans of fluorescence intensities is indicated. These scans are shown on the right. Exposure time for both channels is 100 ms. Frame-to-frame interval is 2 s. Bar, 10 µm.

Acknowledgments: We thank Martin Spitaler and his team at the Imaging Facility of the Max Planck Institute for Biochemistry for cooperation, and the Dicty Base for strains. We are grateful to Britta Schroth-Diez, MPI-CBG, Dresden, for cooperation with TIRF imaging and Ayella Maile-Moskowitz for assistance with data analysis. This work was supported by funds of the Max Planck Society.

REFERENCES

1. Schroth-Diez B, Gerwig S, Ecke M, Hegerl R, Diez S, Gerisch G. Propagating waves separate two states of actin organization in living cells. HFSP J. 2009 Dec;3(6):412–27.
2. Bretschneider T, Anderson K, Ecke M, Müller-Taubenberger A, Schroth-Diez B, Ishikawa-Ankerhold HC, et al. The three-dimensional dynamics of actin waves, a model of cytoskeletal self-organization. Biophys J. 2009 Apr;96(7):2888–900.
3. Faix J, Steinmetz M, Boves H, Kammerer RA, Lottspeich F, Mintert U, et al. Cortexillins, major determinants of cell shape and size, are actin-bundling proteins with a parallel coiled-coil tail. Cell. 1996 Aug;86(4):631–42.
4. Srinivasan K, Wright GA, Hames N, Housman M, Roberts A, Aufderheide KJ, et al. Delineating the core regulatory elements crucial for directed cell migration by examining folic-acid-mediated responses. J Cell Sci. 2013 Jan;126(Pt 1):221–33.
5. Jasnin M, Beck F, Ecke M, Fukuda Y, Martinez-Sanchez A, Baumeister W, et al. The Architecture of Traveling Actin Waves Revealed by Cryo-Electron Tomography. Structure. 2019 Jun;S0969-2126(19)30171-6.
6. Gerisch G, Ecke M, Schroth-Diez B, Gerwig S, Engel U, Maddera L, et al. Self-organizing actin waves as planar phagocytic cup structures. Cell Adh Migr. 2009 Oct-Dec;3(4):373–82.
7. Kovari DT, Wei W, Chang P, Toro JS, Beach RF, Chambers D, et al. Frustrated phagocytic spreading of J774A-1 macrophages ends in myosin II-dependent contraction. Biophys J. 2016 Dec;111(12):2698–710.
8. Mularski A, Marie-Anais F, Mazzolini J, Niedergang F. Observing frustrated phagocytosis and phagosome formation and closure using total internal reflection fluorescence microscopy (TIRFM). In: Rousselet G, editor. Methods in Molecular Biology, Macrophages, 1784. NY: Humana Press; 2018. pp.165-175.
9. Maxson ME, Naj X, O'Meara TR, Plumb JD, Cowen LE, Grinstein S. Integrin-based diffusion barrier separates membrane domains enabling the formation of microbiostatic frustrated phagosomes. Elife. 2018 Mar;7:e34798.
10. Bloomfield G, Traynor D, Sander SP, Veltman DM, Pachebat JA, Kay RR. Neurofibromin controls macropinocytosis and phagocytosis in Dictyostelium. Elife. 2015 Mar;4:e04940.
11. Mahalingam M. NF1 and neurofibromin: emerging players in the genetic landscape of desmoplastic melanoma. Adv Anat Pathol. 2017 Jan;24(1):1–14.
12. Artemenko Y, Lampert TJ, Devreotes PN. Moving towards a paradigm: common mechanisms of chemotactic signaling in Dictyostelium and mammalian leukocytes. Cell Mol Life Sci. 2014 Oct;71(19):3711–47.
13. Wang MJ, Artemenko Y, Cai WJ, Iglesias PA, Devreotes PN. The directional response of chemotactic cells depends on a balance between cytoskeletal architecture and the external gradient. Cell Rep. 2014 Nov;9(3):1110–21.
14. Dunn JD, Bosmani C, Barisch C, Raykov L, Lefrançois LH, Cardenal-Muñoz E, et al. Eat Prey, Live: Dictyostelium discoideum As a Model for Cell-Autonomous Defenses. Front Immunol. 2018;8(1906).
15. Bloomfield G, Kay RR. Uses and abuses of macropinocytosis. J Cell Sci. 2016 Jul;129(14):2697–705.
16. Williams Thomas D, Paschke Peggy I, Kay Robert R. Function of small GTPases in Dictyostelium macropinocytosis. Philosophical Transactions of the Royal Society B: Biological Sciences. 2019;374(1765):20180150.
17. Müller-Taubenberger A, Kortholt A, Eichinger L. Simple system—substantial share: the use of Dictyostelium in cell biology and molecular medicine. Eur J Cell Biol. 2013 Feb;92(2):45–53.
18. McLaren MD, Mathavarajah S, Huber RJ. Recent insights into NCL protein function using the model organism Dictyostelium discoideum. Cells. 2019 Feb;8(2):E115.
19. Phillips JE, Gomer RH. Partial genetic suppression of a loss-of-function mutant of the neuronal ceroid lipofuscinosis-associated protease TPP1 in Dictyostelium discoideum. Dis Model Mech. 2015 Feb;8(2):147–56.
20. Stumpf M, Müller R, Gaßen B, Wehrstedt R, Fey P, Karow MA, et al. A tripeptidyl peptidase 1 is a binding partner of the Golgi pH regulator (GPHR) in Dictyostelium. Dis Model Mech. 2017 Jul;10(7):897–907.
21. Vetter IR, Wittinghofer A. The guanine nucleotide-binding switch in three dimensions. Science. 2001 Nov;294(5545):1299–304.
22. Waters AM, Der CJ. KRAS: The Critical Driver and Therapeutic Target for Pancreatic Cancer. Cold Spring Harb Perspect Med. 2018;8(9).
23. Kae H, Lim CJ, Spiegelman GB, Weeks G. Chemoattractant-induced Ras activation during Dictyostelium aggregation. EMBO Rep. 2004 Jun;5(6):602–6.
24. Graziano BR, Gong D, Anderson KE, Pipathsouk A, Goldberg AR, Weiner OD. A module for Rac temporal signal integration revealed with optogenetics. J Cell Biol. 2017 Aug;216(8):2515–31.
25. Parent CA, Devreotes PN. A cell's sense of direction. Science. 1999 Apr;284(5415):765–70.
26. Clarke M, Engel U, Giorgione J, Müller-Taubenberger A, Prassler J, Veltman D, et al. Curvature recognition and force generation in phagocytosis. BMC Biol. 2010 Dec;8:154.
27. Ostrowski PP, Freeman SA, Fairn G, Grinstein S. Dynamic Podosome-Like Structures in Nascent Phagosomes Are Coordinated by Phosphoinositides. Dev Cell. 2019 Jun;S1534-5807(19)30426-5.
28. Carrera AC, Anderson R. The cell biology behind the oncogenic PIP3 lipids. J Cell Sci. 2019 Jan;132(1):jcs228395.
29. Khalil BD, Hsueh C, Cao Y, Abi Saab WF, Wang Y, Condeelis JS, et al. GPCR Signaling Mediates Tumor Metastasis via PI3Kβ. Cancer Res. 2016 May;76(10):2944–53.
30. Papa A, Wan L, Bonora M, Salmena L, Song MS, Hobbs RM, et al. Cancer-associated PTEN mutants act in a dom-

inant-negative manner to suppress PTEN protein function. Cell. 2014 Apr;157(3):595–610.
31. Yehia L, Ngeow J, Eng C. PTEN-opathies: from biological insights to evidence-based precision medicine. J Clin Invest. 2019 Feb;129(2):452–64.
32. Chen C-Y, Chen J, He L, Stiles BL. PTEN: Tumor Suppressor and Metabolic Regulator. Front Endocrinol (Lausanne). 2018;9(338).
33. Nguyen HN, Yang JM Jr, Rahdar M, Keniry M, Swaney KF, Parsons R, et al. A new class of cancer-associated PTEN mutations defined by membrane translocation defects. Oncogene. 2015 Jul;34(28):3737–43.
34. Hartman MA, Finan D, Sivaramakrishnan S, Spudich JA. Principles of unconventional myosin function and targeting. Annu Rev Cell Dev Biol. 2011;27(1):133–55.
35. Bond LM, Tumbarello DA, Kendrick-Jones J, Buss F. Small-molecule inhibitors of myosin proteins. Future Med Chem. 2013 Jan;5(1):41–52.
36. Preller M, Manstein DJ. Myosin structure, allostery, and mechano-chemistry. Structure. 2013 Nov;21(11):1911–22.
37. Kollmar M. Thirteen is enough: the myosins of Dictyostelium discoideum and their light chains. BMC Genomics. 2006 Jul;7:183.
38. Jung G, Wu X, Hammer JA 3rd. Dictyostelium mutants lacking multiple classic myosin I isoforms reveal combinations of shared and distinct functions. J Cell Biol. 1996 Apr;133(2):305–23.
39. Brzeska H, Guag J, Preston GM, Titus MA, Korn ED. Molecular basis of dynamic relocalization of Dictyostelium myosin IB. J Biol Chem. 2012 Apr;287(18):14923–36.
40. de Hostos EL, Bradtke B, Lottspeich F, Guggenheim R, Gerisch G. Coronin, an actin binding protein of Dictyostelium discoideum localized to cell surface projections, has sequence similarities to G protein beta subunits. EMBO J. 1991 Dec;10(13):4097–104.
41. de Hostos EL, Rehfuess C, Bradtke B, Waddell DR, Albrecht R, Murphy J, et al. Dictyostelium mutants lacking the cytoskeletal protein coronin are defective in cytokinesis and cell motility. J Cell Biol. 1993 Jan;120(1):163–73.
42. Maniak M, Rauchenberger R, Albrecht R, Murphy J, Gerisch G. Coronin involved in phagocytosis: dynamics of particle-induced relocalization visualized by a green fluorescent protein tag. Cell. 1995 Dec;83(6):915–24.
43. Appleton BA, Wu P, Wiesmann C. The crystal structure of murine coronin-1: a regulator of actin cytoskeletal dynamics in lymphocytes. Structure. 2006 Jan;14(1):87–96.
44. Ishikawa-Ankerhold HC, Gerisch G, Müller-Taubenberger A. Genetic evidence for concerted control of actin dynamics in cytokinesis, endocytic traffic, and cell motility by coronin and Aip1. Cytoskeleton (Hoboken). 2010 Jul;67(7):442–55.
45. Gandhi M, Achard V, Blanchoin L, Goode BL. Coronin switches roles in actin disassembly depending on the nucleotide state of actin. Mol Cell. 2009 May;34(3):364–74.
46. Liu X, Gao Y, Lin X, Li L, Han X, Liu J. The coronin family and human disease. Curr Protein Pept Sci. 2016;17(6):603–11.
47. Mori M, Mode R, Pieters J. From phagocytes to immune defense: roles for coronin proteins in Dictyostelium and mammalian immunity. Front Cell Infect Microbiol. 2018 Mar;8:77.
48. Jayachandran R, Gumienny A, Bolinger B, Ruehl S, Lang MJ, Fucile G, et al. Disruption of coronin 1 signaling in T cells promotes allograft tolerance while maintaining anti-pathogen immunity. Immunity. 2019;50(1):152-65 e8.
49. Ford ML. Coronin-1, king of alloimmunity. Immunity. 2019 Jan;50(1):3–5.
50. Martorella M, Barford K, Winkler B, Deppmann CD. Emergent role of coronin-1a in neuronal signaling. Vitam Horm. 2017;104:113–31.
51. Vazquez F, Matsuoka S, Sellers WR, Yanagida T, Ueda M, Devreotes PN. Tumor suppressor PTEN acts through dynamic interaction with the plasma membrane. Proc Natl Acad Sci U S A. 2006 Mar;103(10):3633–8.
52. Fukushima S, Matsuoka S, Ueda M. Excitable dynamics of Ras triggers spontaneous symmetry breaking of PIP3 signaling in motile cells. J Cell Sci. 2019 Mar;132(5):-jcs224121.
53. Gerhardt M, Ecke M, Walz M, Stengl A, Beta C, Gerisch G. Actin and PIP3 waves in giant cells reveal the inherent length scale of an excited state. J Cell Sci. 2014 Oct;127(Pt 20):4507–17.
54. Brzeska H, Pridham K, Chery G, Titus MA, Korn ED. The association of myosin IB with actin waves in Dictyostelium requires both the plasma membrane-binding site and actin-binding region in the myosin tail. PLoS One. 2014 Apr;9(4):e94306.
55. Clarke M, Engel U, Giorgione J, Müller-Taubenberger A, Prassler J, Veltman D, et al. Curvature recognition and force generation in phagocytosis. BMC Biol. 2010 Dec;8:154.
56. Clarke M, Müller-Taubenberger A, Anderson KI, Engel U, Gerisch G. Mechanically induced actin-mediated rocketing of phagosomes. Mol Biol Cell. 2006 Nov;17(11):4866–75.
57. Etzrodt M, Ishikawa HC, Dalous J, Müller-Taubenberger A, Bretschneider T, Gerisch G. Time-resolved responses to chemoattractant, characteristic of the front and tail of Dictyostelium cells. FEBS Lett. 2006 Dec;580(28-29):6707–13.
58. Heinrich D, Youssef S, Schroth-Diez B, Engel U, Aydin D, Blümmel J, et al. Actin-cytoskeleton dynamics in non-monotonic cell spreading. Cell Adh Migr. 2008 Apr-May;2(2):58–68.
59. Gerisch G, Schroth-Diez B, Müller-Taubenberger A, Ecke M. PIP3 waves and PTEN dynamics in the emergence of cell polarity. Biophys J. 2012 Sep;103(6):1170–8.
60. Gerisch G, Bretschneider T, Müller-Taubenberger A, Simmeth E, Ecke M, Diez S, et al. Mobile actin clusters and traveling waves in cells recovering from actin depolymerization. Biophys J. 2004 Nov;87(5):3493–503.
61. Heinrich D, Ecke M, Jasnin M, Engel U, Gerisch G. Reversible membrane pearling in live cells upon destruction of the actin cortex. Biophys J. 2014 Mar;106(5):1079–91.
62. Jasnin M, Ecke M, Baumeister W, Gerisch G. Actin organization in cells responding to a perforated surface, revealed by live imaging and cryo-electron tomography. Structure. 2016 Jul;24(7):1031–43.
63. Eddy RJ, Weidmann MD, Sharma VP, Condeelis JS. Tumor cell invadopodia: invasive protrusions that orchestrate metastasis. Trends Cell Biol. 2017 Aug;27(8):595–607.

64. Williams KC, Cepeda MA, Javed S, Searle K, Parkins KM, Makela AV, et al. Invadopodia are chemosensing protrusions that guide cancer cell extravasation to promote brain tropism in metastasis. Oncogene. 2019 May;38(19):3598–615.
65. Helenius J, Ecke M, Müller DJ, Gerisch G. Oscillatory switches of dorso-ventral polarity in cells confined between two surfaces. Biophys J. 2018 Jul;115(1):150–62.
66. Sasaki AT, Chun C, Takeda K, Firtel RA. Localized Ras signaling at the leading edge regulates PI3K, cell polarity, and directional cell movement. J Cell Biol. 2004 Nov;167(3):505–18.
67. Li X, Edwards M, Swaney KF, Singh N, Bhattacharya S, Borleis J, et al. Mutually inhibitory Ras-PI(3,4)P2 feedback loops mediate cell migration. Proc Natl Acad Sci U S A. 2018 Sep;115(39):E9125–34.
68. Knoch F, Tarantola M, Bodenschatz E, Rappel WJ. Modeling self-organized spatio-temporal patterns of PIP_3 and PTEN during spontaneous cell polarization. Phys Biol. 2014 Aug;11(4):046002.
69. Lusche DF, Wessels D, Richardson NA, Russell KB, Hanson BM, Soll BA, et al. PTEN redundancy: overexpressing lpten, a homolog of Dictyostelium discoideum ptenA, the ortholog of human PTEN, rescues all behavioral defects of the mutant ptenA-. PLoS One. 2014 Sep;9(9):e108495.
70. Sasaki AT, Janetopoulos C, Lee S, Charest PG, Takeda K, Sundheimer LW, et al. G protein-independent Ras/PI3K/F-actin circuit regulates basic cell motility. J Cell Biol. 2007 Jul;178(2):185–91.
71. Vazquez F, Devreotes P. Regulation of PTEN function as a PIP3 gatekeeper through membrane interaction. Cell Cycle. 2006 Jul;5(14):1523–7.
72. Fischer M, Haase I, Simmeth E, Gerisch G, Müller-Taubenberger A. A brilliant monomeric red fluorescent protein to visualize cytoskeleton dynamics in Dictyostelium. FEBS Lett. 2004 Nov;577(1-2):227–32.
73. Schneider N, Weber I, Faix J, Prassler J, Müller-Taubenberger A, Köhler J, et al. A Lim protein involved in the progression of cytokinesis and regulation of the mitotic spindle. Cell Motil Cytoskeleton. 2003 Oct;56(2):130–9.
74. de Rooij J, Bos JL. Minimal Ras-binding domain of Raf1 can be used as an activation-specific probe for Ras. Oncogene. 1997 Feb;14(5):623–5.
75. Müller-Taubenberger A, Ishikawa-Ankerhold HC. Fluorescent reporters and methods to analyze fluorescent signals. In: Eichinger LR, editor. Dictyostelium discoideum Protocols. Methods in Molecular Biology (Methods and Protocols). 983. Totowa (NJ): Humana Press; 2013. pp. 93–112.
76. Iijima M, Devreotes P. Tumor suppressor PTEN mediates sensing of chemoattractant gradients. Cell. 2002 May;109(5):599–610.
77. Hoeller O, Kay RR. Chemotaxis in the absence of PIP3 gradients. Curr Biol. 2007 May;17(9):813–7.
78. Fey P, Dodson RJ, Basu S, Chisholm RL. One stop shop for everything Dictyostelium: dictyBase and the Dicty Stock Center in 2012. Methods Mol Biol. 2013;983:59–92.
79. Schindelin J, Arganda-Carreras I, Frise E, Kaynig V, Longair M, Pietzsch T, et al. Fiji: an open-source platform for biological-image analysis. Nat Methods. 2012 Jun;9(7):676–82.
80. Hoeller O, Bolourani P, Clark J, Stephens LR, Hawkins PT, Weiner OD, et al. Two distinct functions for PI3-kinases in macropinocytosis. J Cell Sci. 2013 Sep;126(Pt 18):4296–307.
81. van Haastert PJ, Keizer-Gunnink I, Kortholt A. Coupled excitable Ras and F-actin activation mediates spontaneous pseudopod formation and directed cell movement. Mol Biol Cell. 2017 Apr;28(7):922–34.